OFFICE OF NAVAL RESEARCH

GRANT N0001498AF00002

PR Number 98PR01192-00

Technical Report No. 18

# NMR, DSC and High Pressure Electrical Conductivity Studies on Liquid and Hybrid Electrolytes

Prepared for publication in the Journal of Power Sources

by

P. E. Stallworth, J. J. Fontanella, M. C. Wintersgill
Christopher D. Scheidler, Jeffrey J. Immel,
Physics Department
U. S. Naval Academy
Annapolis, MD 21402-5026

S. G. Greenbaum
Hunter College of the CUNY
New York, NY 10012

A. S. Gozdz
Bellcore
331 Newman Springs Road
Red Bank, NJ 07701

1 July 1998

# REPORT DOCUMENTATION PAGE

Form Approved
OMB No. 0704-0188



**1. AGENCY USE ONLY** *(Leave blank)*

**2. REPORT DATE**
July 1, 1998

**3. REPORT TYPE AND DATES COVERED**
Technical Report 6/1/97 - 5/31/98

**4. TITLE AND SUBTITLE**
NMR, DSC and High Pressure Electrical Conductivity Studies on Liquid and Hybrid Electrolytes

**5. FUNDING NUMBERS**
Grant:
N00014-98-WR-20007
PR Number:
96PRO-3804
Richard T. Carlin

**6. AUTHOR(S)**
P. E. Stallworth, J. J. Fontanella, M. C. Wintersgill, C. D. Scheidler, J. J. Immel, S. G. Greenbaum and A. S. Gozdz

**7. PERFORMING ORGANIZATION NAME(S) AND ADDRESS(ES)**
United States Naval Academy
Physics Department
Annapolis, MD 21402

**8. PERFORMING ORGANIZATION REPORT NUMBER**
Technical Report #18

**9. SPONSORING/MONITORING AGENCY NAME(S) AND ADDRESS(ES)**
Office of Naval Research
Chemistry Division
800 North Quincy Street
Arlington, VA 22217-5660

**10. SPONSORING/MONITORING AGENCY REPORT NUMBER**

**11. SUPPLEMENTARY NOTES**
Prepared for Publication in J. of Power Sources

**12a. DISTRIBUTION/AVAILABILITY STATEMENT**
Reproduction in whole or in part is permitted for any purpose of the United States Government. This document has been approved for public release and sale; its distribution is unlimited

**12b. DISTRIBUTION CODE**

**13. ABSTRACT** *(Maximum 200 words)*
Electrical conductivity, DSC and $^7Li$ NMR studies have been carried out on liquid electrolytes such as EC:PC and EC:DMC containing $LiPF_6$ (and $LiCF_3SO_3$ for NMR) and films plasticized using the same liquid electrolytes. The films are based on poly(vinylidene fluoride) copolymerized with hexafluoropropylene and contain fumed silica. All measurements were carried out at atmospheric pressure from room temperature to about 120K and the electrical conductivity studies were performed at room temperature at pressures up to 0.3 GPa. The liquids and hybrid electrolytes are similar in that the electrical conductivity of the EC:PC based materials exhibits VTF behaviour while that for the EC:DMC based materials does not. Further, the glass transition temperatures as determined from NMR, DSC and electrical conductivity measurements are about the same for the liquids and hybrid electrolytes. However, substantial differences are found. The electrical conductivity of the hybrid electrolytes at room temperature is lower than expected and, more importantly, the relative change of conductivity with pressure is larger than for the liquids. In addition, above the glass transition temperature, the NMR $T_1$ values are smaller for the plasticized films than for the liquids while at both low and high temperature the NMR linewidths are larger. Consequently, it is concluded that significant solid matrix-lithium ion interactions take place.

**14. SUBJECT TERMS**
Electrical Conductivity, Nuclear Magnetic Resonance, Lithium Electrolytes, Activation Volume, High Pressure

**15. NUMBER OF PAGES**
29

**16. PRICE CODE**

| 17. SECURITY CLASSIFICATION OF REPORT | 18. SECURITY CLASSIFICATION OF THIS PAGE | 19. SECURITY CLASSIFICATION OF ABSTRACT | 20. LIMITATION OF ABSTRACT |
|---|---|---|---|
| UNCLASSIFIED | UNCLASSIFIED | UNCLASSFIED | |

# NMR, DSC AND HIGH PRESSURE ELECTRICAL CONDUCTIVITY STUDIES ON LIQUID AND HYBRID ELECTROLYTES

P. E. Stallworth,[a] J. J. Fontanella,[a] M. C. Wintersgill,[a] Christopher D. Scheidler,[a] Jeffrey J. Immel,[a] S. G. Greenbaum,[b] A. S. Gozdz[c]

a. Physics Department, U.S. Naval Academy, Annapolis, MD 21402-5026, USA
b. Hunter College of the CUNY, New York, NY 10012, USA
c. Bellcore, 331 Newman Springs Road, Red Bank, NJ 07701, USA

Electrical conductivity, DSC and $^{7}Li$ NMR studies have been carried out on liquid electrolytes such as EC:PC and EC:DMC containing $LiPF_6$ (and $LiCF_3SO_3$ for NMR) and films plasticized using the same liquid electrolytes. The films are based on poly(vinylidene fluoride) copolymerized with hexafluoropropylene and contain fumed silica. All measurements were carried out at atmospheric pressure from room temperature to about 120K and the electrical conductivity studies were performed at room temperature at pressures up to 0.3 GPa. The liquids and hybrid electrolytes are similar in that the electrical conductivity of the EC:PC based substances exhibits VTF behaviour while that for the EC:DMC based substances does not. Further, the glass transition temperatures as determined from NMR, DSC and electrical conductivity measurements are about the same for the liquids and hybrid electrolytes. However, substantial differences are found. The electrical conductivity of the hybrid electrolytes at room temperature is lower than expected and, more importantly, the relative change of conductivity with pressure is larger than for the liquids. In addition, above the glass transition temperature, the NMR $T_1$ values are smaller for the hybrid electrolytes than for the liquids while at both low and high temperature the NMR linewidths are larger. Consequently, it is concluded that significant solid matrix-lithium ion interactions take place.

**Keywords**: Electrical Conductivity, Nuclear Magnetic Resonance, Lithium Electrolytes, Activation Volume, High Pressure

## INTRODUCTION

Rechargeable lithium batteries with hybrid polymeric electrolytes are currently being widely studied [1-13] (This list of references is representative rather than comprehensive.) One polymer of interest is poly(vinylidene fluoride) (PVdF). Early work on PVdF includes that of Feuillade et al. [14], Tsuchida et al. [15] and Tsunemi et al. [16]. More recently, Jiang et al. have reported results on this system [17].

In order to learn more about hybrid electrolytes, differential scanning calorimetry (DSC), electrical conductivity and nuclear magnetic resonance (NMR) studies have been undertaken. The electrical conductivity studies were extended to high pressures. The liquids studied include $LiPF_6$ or $LiCF_3SO_3$ dissolved in various solutions of ethylene carbonate (EC), propylene carbonate (PC) or dimethyl carbonate (DMC). In addition, films were studied which were composed of fumed silica dispersed in poly(vinylidene fluoride) copolymerized with hexafluoropropylene and which were plasticized using the same liquid electrolytes.

Despite the complexity of the system, relatively simple behaviour is observed. For example, many of the new results are interpreted in terms of crystallization and glass formation. These occur to varying degrees depending upon the details of the experiment performed. Further, all behaviour is consistent with the properties of the constituents. For example, PC is a well known glass-former while EC and DMC crystallize easily and combinations of these behave accordingly. Complications arise because PC can crystallize and EC and DMC can be part of amorphous systems. In addition, inclusion of the polymer and silica in the system produces

subtle, yet important effects. In the present paper electrical conductivity, NMR and DSC measurements are used to elucidate the behaviour of the system.

## EXPERIMENTAL

Two commercial liquids were obtained from EM Industries. The first was a 1 M solution of $LiPF_6$ dissolved in 1:1 volume EC:PC, and the second sample was also a 1 M concentration of the salt, but dissolved in a 1:1 volume EC:DMC. The only liquids prepared in the laboratory were a 1:1 solution of EC:PC, 1:1 solution of EC:DMC and 1 M $LiCF_3SO_3$ in 1:1 EC:PC. These were prepared using 99.7% anhydrous PC, 99% DMC and 98% EC which were obtained from from Aldrich Chemical Company and $LiCF_3SO_3$ from Alfa Aesar. The electrolytes were then used to saturate silica-containing polymer films based on poly(vinylidene fluoride) copolymerized with hexafluoropropylene. Noticeable swelling of the films occurred during plasticization and mass increases of about 100% were typical. Prior to measurement, the plasticized films were removed from the liquids and lightly patted with a tissue to remove the surface liquid. All sample preparation and subsequent loading of the samples into various sample holders were carrried out in a Vac Atmospheres glove box with less than 0.08 ppm water.

For the electrical measurements, the liquids were placed in Teflon™ coated Tygon™ tubing. One end of the tube was plugged with a gold-coated stainless steel electrode and sealed using a modified SwageLok™ fitting. The liquid to be examined was then placed in the tubing with an eye dropper, and other end of the sample was then plugged with another electrode assembly. A similar arrangement was used for the plasticized films which were measured along the plane of the samples.

The electrical conductivity of the samples at various temperatures was determined by connecting the samples to the cold finger of a Cryogenics Associates CT-14 cryostat. Temperature control was achieved using a Lake Shore Cryotronics DRC-82 temperature controller. This is the same system used previously for a variety of measurements [18-22]. For the high pressure measurements, the samples were connected to the closure plug of the high pressure vessel used previously to measure the effect of high pressure on the electrical conductivity of ion conducting polymers [18,21,23-27]. For both the variable pressure and temperature measurements, the equivalent parallel capacitance and resistance of the sample were then determined using either a CGA-83 capacitance measuring assembly or a Hewlett Packard 4194A Impedance/Gain-Phase Analyzer which achieve a combined frequency range of 10 Hz to 100 MHz. All data were then transformed to the complex impedance, $Z^* = Z' - jZ''$.

For the NMR measurements, the samples were sealed inside 5 mm diameter Pyrex™ tubes. The $^7Li$ NMR measurements were carried out at ambient pressure using a Chemagnetics CMX-300 spectrometer operating at a frequency of 116 MHz. Dry nitrogen gas was used as a purge. Linewidths were determined from Fourier transformed single pulse responses and spin-lattice relaxation times were obtained from exponential relaxation profiles utilizing a saturation-recovery pulse sequence.

The DSC measurements were carried out at a scanning rate of 10 K/min using a DuPont Thermal Analyst 2100 with a 910 Cell Base. The DSC measurements for the salt-containing liquids were made using both gold and anodized aluminum pans. No difference was found.

## RESULTS

For all electrical experiments a complex impedance diagram consisting of a slightly depressed semicircular arc and slanted line was observed. Those features are usually observed in ion conducting systems such as solvent-free ion conducting polymers with blocking electrodes [18-22]. The bulk resistance, R, was obtained from the intercept of the arc (or position of the minimum value of Z") or slanted line with the Z' axis. The conductance, G=1/R, was calculated from the intercept. In the case of the room temperature, atmospheric pressure data, the conductance was transformed to the electrical conductivity, $\sigma$, via the usual equation:

$$\sigma = GL/A \qquad (1)$$

where A is the area of the sampleand L is the length. The results are listed in Table 1.

It was found that the EC:DMC:$LiPF_6$ and EC:PC:$LiPF_6$ had conductivities of about 11.5 and 6.8 mS/cm, respectively, at room temperature (approximately 23°C). The value for EC:PC:$LiPF_6$ is in good agreement with the value of 6.56 mS/cm reported for 1 M $LiPF_6$ in 50:50 vol-% EC:PC at 20°C [28]. The conductivity for each associated hybrid electrolyte is lower.

Values of the electrical conductivity at other temperatures and approximately atmospheric pressure were obtained by assuming that the relative change in electrical conductivity is the same as the relative change in electrical conductance, i.e. no correction was made for changes in the dimensions of the sample. The results for the variation of the conductivity with temperature for the liquid and hybrid electrolytes are shown in Figs. 1 and 2, respectively.

The results for the variation of the conductance with pressure at room temperature are shown in Fig. 3. Straight lines were best-fitted to the data and the resultant slopes and intercepts are listed in Table 1. The pressure variation of the electrical conductivity can be calculated from:

$$\left(\frac{\partial \ln \sigma}{\partial p}\right)_T = \left(\frac{\partial \ln G}{\partial p}\right)_T + \frac{\chi_T}{3} \qquad (2)$$

where $\chi_T$ is the isothermal compressibility. The compressibility for these materials does not seem to be available. However, the compressibility for most liquids is on the order of 0.8-1.2 $GPa^{-1}$ [29]. Consequently, an approximate correction of $\chi_T/3 \cong$ 0.3 $GPa^{-1}$ was applied to the data and the results are listed in Table 1.

The results of the DSC runs are shown in Figs. 4-6. The $^7Li$ NMR linewidth results are shown in Fig. 7 and the $T_1$ data are shown in Fig. 8.

## DISCUSSION

It is clear from Figs. 1 and 2 that the temperature variation of the electrical conductivity of both EC:PC:$LiPF_6$ and the related hybrid electrolyte is significantly different from that of the EC:DMC:$LiPF_6$-based substances. While the electrical conductivity of the former exhibits a smooth variation with temperature, the latter does not, with the EC:DMC:$LiPF_6$ and associated hybrid electrolyte showing a precipitous drop in the vicinity of 250K. This behaviour was reproducible under the conditions of the electrical conductivity measurements. However, as discussed below, a discontinuity at 250K is not observed in the NMR measurements and, while an event is observed in the vicinity of 250K in the DSC thermograms other features are also observed.

The interpretation of the difference between the two systems is that, under the conditions of the electrical conductivity studies, as temperature is lowered EC:DMC:$LiPF_6$ and the related hybrid electrolyte undergo crystallization in the vicinity of 250K while EC:PC:$LiPF_6$-based substances do not, the latter being a glass-forming liquid. This interpretation is consistent with the DSC results shown in Figs. 4-6. It is apparent from Figs. 4 and 6 that all EC- and DMC-based substances exhibit a strong endothermic event typical of melting and for EC:DMC:$LiPF_6$, the melting is observed in the vicinity of 250K. The position of the endotherm varies over a range of about 10$^o$C depending upon the conditions of the experiment, cooling rate, etc. Obviously, the DMC-based substances have a tendency to crystallize.

On the other hand, as is apparent from Figs. 5 and 6, all of the PC based materials show a strong endotherm typical of a glass transition. For EC:PC:$LiPF_6$ and the related hybrid electrolyte the glass transition is observed at about -90$^o$C. This is consistent with the data shown in Fig. 7 where it is seen that the $^7$Li NMR linewidth for the EC:PC:$LiPF_6$-based substances exhibits a rapid rise as the temperature is reduced below about 190K. This result reflects a similar change in the dynamics of the solvated lithium ions in the liquid and hybrid electrolytes as the temperature is reduced below $T_g$.

However, at about 0$^o$C, both EC:PC:$LiPF_6$ and the related hybrid electrolyte also exhibit a DSC endotherm typical of melting. This endotherm is preceded by an exotherm which probably represents crystallization. Such an event is not reflected in either the electrical conductivity or NMR data. That is not surprising since both the electrical conductivity and NMR experiments are carried out at various temperatures achieved by slowly cooling the sample to the desired temperature then equilibrating so that the data are taken isothermally. The DSC data, on the other hand, are taken while the temperature is increasing at 10 K/min.

Next, a weak glass transition is observed for both EC:DMC:$LiPF_6$ and the associated hybrid electrolyte even though EC:DMC appears to be totally crystalline. This is not an unknown phenomenon since in PEO, for example, $NaCF_3SO_3$ and NaI have been observed to suppress crystallinity in favor of an amorphous structure [27]. It is significant that $T_g$ occurs at a higher temperature both in EC:DMC:$LiPF_6$ and the related hybrid electrolyte than for the EC:PC:$LiPF_6$-based substances since $T_g$ varies from about -67 to about -76°C. This is confirmed by the $^7$Li NMR linewidth data shown in Fig. 7. Specifically, while the EC:PC:$LiPF_6$-based substances exhibit a rapid rise in the linewidth when the temperature is reduced below about -90°C, the rise occurs at about 20°C higher for EC:DMC:$LiPF_6$ and about 10°C higher for the associated hybrid electrolyte.

The smooth variation of the electrical conductivity with temperature observed for EC:PC:$LiPF_6$ is not surprising since EC:PC containing other salts has been shown to be a glass-forming liquid and the related smooth variation of such properties as viscosity, electrical conductivity or dielectric relaxation times for one of the constituents, PC, is well-documented [30-37]. A quantitative treatment can be given in terms of the VTF [38] equation:

$$\sigma = \sigma_0 \exp\left(\frac{-B}{T - T_0}\right) \qquad (3)$$

or the modified VTF equation:

$$\sigma = \frac{A}{\sqrt{T}} \exp\left(\frac{-B'}{T - T_0'}\right) \qquad (4)$$

A non-linear least squares procedure was carried out as described elsewhere [39]. The resultant best-fit parameters are listed in Table 2 and the best-fit curves are shown in Figs. 1 and 2.

It is interesting that the values of $T_0$ or $T_0'$, the "ideal glass transition temperatures" for EC:PC:$LiPF_6$ and the associated hybrid electrolyte are about 160K. This is consistent with $T_g$ from both DSC ($T_g$ = 183K) and NMR ($T_g$ = 190K) since $T_0$ and $T_0'$ are usually 20-50°C below $T_g$ [18,20-23,26,27,35]. Further insight can be obtained by comparing the VTF results to a similar treatment of structural relaxation times and viscosity. Still other information can be obtained by applying both the formalism of Williams, Landau and Ferry [35,40], which is mathematically equivalent to the VTF equation, and the theory of Bendler and Shlesinger [41] to the data. Those discussions are given elsewhere [36].

The result that the values of the transition temperatures for EC:PC:$LiPF_6$ and the related hybrid electrolyte are approximately the same is another indication that the liquid in the hybrid electrolyte is similar to the pure liquid. In fact, as is apparent from Figs. 5 and 6, the DSC thermograms for EC:PC:$LiPF_6$ and its hybrid electrolyte are essentially identical. However, the DSC data shown in Figs. 4 and 6 show that EC:DMC:$LiPF_6$ and its hybrid electrolyte are different. Even though the glass transition temperatures occur at approximately the same position and there is an exotherm at about the same temperature (-40°C) in both substances, EC:DMC:$LiPF_6$ exhibits a second high temperature exothem (-30°C) and melting occurs at a different temperature. This behaviour is not surprising since it is expected that crystallization and melting would be particularly sensitive to the environment of the liquid.

However, there are other results which show differences between the bulk liquids and the liquid in the hybrid electrolytes. First, it is clear that the value of the electrical conductivity of the hybrid electrolyte cannot be explained by assuming

that the film is an inert insulating material since a detailed analysis of a similar system showed that the hybrid electrolyte has a lower conductivity than that predicted by the Bruggeman formula [3]. One explanation is that the electrical conductivity of the liquid in the plasticized film is lower than that of the bulk liquid. Evidence that this is probably the case is as follows.

For temperatures greater than 200 K, the NMR linewidths (full-width at half-maximum) are 300-400 Hz for both hybrid electrolytes and about 60-160 Hz for the liquids. In that temperature range, the line broadening due to quadrupolar interactions can be neglected and differences in $^{7}Li$ linewidths between the hybrid electrolyte and the liquid can be attributed to a combination of magnetic dipolar interactions with protons, $^{7}Li$, $^{19}F$ and $^{31}P$ nuclei. The smaller linewidths for the liquids reflect the efficient averaging of the dipolar interaction due to rapid lithium ion motion. Therefore, hindered motions of the lithium ions produce relatively larger linewidths as observed with the hybrid electrolytes.

As the temperature is reduced below 190 K, the distinctions between the liquids and hybrid electrolytes become more apparent. The "rigid-lattice" linewidths (limiting values) are slightly larger for the hybrid electrolytes than for the liquids (about 4 kHz). The effect of the film is to increase the magnetic dipole contribution on the $^{7}Li$ line. The general shape of the low-temperature $^{7}Li$ responses are the same for all samples revealing the 1/2 to -1/2 central transition flanked by the broadened satellite transitions; therefore, the lithium chemical environments are very similar in both the liquids and hybrid electrolytes. Lithium ions probably do not bond directly to the film. Instead the solid matrix acts indirectly to modify the structure and/or dynamics of the solvation sphere (units of EC:PC, EC:DMC and anion) about the lithium ions. The details of the interaction are not completely known; but, since the magnetic dipolar contribution goes as $r^{-3}$ (r is the dipole-dipole distance) it appears that the film causes the lithium ions to be

more "tightly" bound to their solvation spheres or allows for the anion to reside in closer proximity to the lithium ions.

Comparison of the low-temperature linewidth behavior shown in Fig. 7 reveals a 1.5 kHz difference between EC:PC:$LiPF_6$ and EC:PC:$LiCF_3SO_3$. This result indicates that significant anion effects exist. Based upon the number of interacting spins, it is reasonable that the $PF_6$ anion contributes more to the magnetic dipolar interaction than the $CF_3SO_3$ anion. It is also plausible that residual motions of the solvated lithium species exist when $CF_3SO_3$ anions are present as opposed to $PF_6$ anions. These differences would arise from the lithium cation association competition between anions and EC:PC solvent. It must be noted that previous $^7Li$-$^{19}F$ decoupling studies of EC:PC:$LiAsF_6$ in PMMA show that the dipolar broadening contribution to the $^7Li$ NMR line by surrounding fluorine nuclei is small, suggesting that $AsF_6$ anions are in rapid motion and/or remotely located such that the lithium ions are solvated by (non-fluorinated) EC and PC molecules [42]. On the other hand, dipolar interactions between $^7Li$ and $^{19}F$ have been reported for polyethers [43] and PAN [44] complexed with $LiBF_4$, indicating that for these materials the lithium ions reside near to their anion counterparts. Clearly there are conflicting opinions for related phenomena in electrolyte gels but the situation needs to be clarified and understood in the context of hybrid electrolytes.

Further differences between the liquids and hybrid electrolytes are provided by the temperature dependence of the spin-lattice relaxation times, $T_1$. In general, the Arrhenius $T_1$ contours are higher for the liquid samples than for the associated hybrid electrolytes (Fig. 8). This suggests that, for dynamics on the order of 100 MHz, the solvated lithium complexes are more tightly held (i.e. their motions are inhibited). This results in the lower $T_1$ values in the solid matrix over the liquids. The solvent effect, observed in the linewidth behavior, is also observed in the $T_1$ data as well. The $T_1$ contours for the EC:DMC-based substances are higher than

the contours for the EC:PC-based substances. Therefore, DMC has the effect of decoupling the lithium ion from the "lattice" so that the nuclei do not relax as effectively as when PC is present. Moreover, the $T_1$ contours for the EC:PC-based liquids and hybrid electrolytes are more broad and U-shaped; whereas, the contours for the EC:DMC-based substances are sharper and V-shaped. This implies that the lithium ion environments in the EC:PC-based substances are more heterogeneous and that correlation times associated with lithium ion motions are more widely distributed. Such behavior is often observed in vitreous and heterogeneous systems and is supported by the fact that EC:PC:$LiPF_6$ forms glasses easily whereas EC:DMC:$LiPF_6$ does not under the experimental conditions employed here.

Anion effects are also present in the $T_1$ results. For temperatures between 200K and 300K the relaxation times for the EC:PC:$LiPF_6$ hybrid electrolyte are over two orders-of-magnitude smaller than for the EC:PC:$LiCF_3SO_3$ hybrid electrolyte. Therefore more efficient relaxational processes are present for the former plasticized film due to the different anion. As mentioned in the linewidth results, the solvated lithium ions are possibly more mobile, with increased $T_1$ values, when the $CF_3SO_3$ anion is present as opposed to the $PF_6$ anion.

The relaxation data do not clearly show abrupt changes near 190 K. The spin-lattice relaxation times describe motions that are of a much higher frequency than those associated with any polymer segmental motions, for example, and the high frequency couplings between the nuclear spin system and the lattice are greatest when the relaxation times are smallest. The $T_1$ minimum for the EC:PC:$LiPF_6$ hybrid electrolyte lies above room temperature and therefore was not observed. This provides evidence that high-frequency ion motions (such as rotations) are more inhibited even at room temperature in this hybrid electrolyte than in any of the liquids or the other plasticized films.

In order to discuss the effect of pressure on the electrical conductivity, the "Arrhenius" activation volume

$$\Delta V = -kT\left(\frac{\partial \ln \sigma}{\partial p}\right)_T \qquad (5)$$

is considered. The values of $\Delta V$, calculated using equation (5), are listed in Table 1. As has been discussed elsewhere [18,25,45], the activation volume as defined above is not strictly correct for materials which exhibit non-Arrhenius behaviour. However, it is a useful quantity for comparison with data in the literature.

The effect of pressure on the electrical conductivity of the liquids is consistent with previous results for related liquids [25]. In the previous work, it was found that the activation volume for EC:DMC in a different ratio (2:1) containing various salts ranged from 11.2 to 12.7 $cm^3$/mol. This overlaps the value of 12.5 $cm^3$/mol observed in the present work for EC:DMC:$LiPF_6$. The value for EC:PC:$LiPF_6$ is somewhat larger at 15.2 $cm^3$/mol. An explanation of the larger value of $\Delta V$ for EC:PC:$LiPF_6$ is that the molecules fill a larger percentage of the available space than in the case of EC:DMC:$LiPF_6$ i.e. there is more free volume in EC:DMC:$LiPF_6$. Therefore, the activation volume is larger because EC:PC:$LiPF_6$ requires more *change* in volume (which the activation volume represents) in order for the ions to migrate. This is also consistent with the electrical conductivity and NMR results. Specifically, from Table 1, the liquid with the larger electrical conductivity exhibits the smaller activation volume. Again, this is reasonable since the interpretation is that the higher electrical conductivity is a result of the extra volume which is available in EC:DMC:$LiPF_6$. It will be of interest to investigate these liquids containing other salts.

The pressure dependence of the electrical conductivity shows a difference between each liquid and the associated hybrid electrolyte since the activation volume for the hybrid electrolyte is slightly larger than for the liquid. The same trend was observed for gel electrolytes based on poly(acrylonitrile) [25]. This difference cannot be accounted for by a geometrical model and thus again represents a fundamental difference between the liquid and liquid in the associated hybrid electrolyte. The reason is that the pressure variation of either the conductance or conductivity (or activation volume which is calculated using the relative change in conductivity) are quoted as a *relative* change and relative changes are independent of the size and shape of the solid matrix provided that they do not change with the application of high pressure. Consequently, the difference in the pressure dependence between the liquids and associated hybrid electrolytes represents evidence for an interaction between the solid matrix and the mobile ions. This is, of course, consistent with the NMR results discussed above.

Next, it is noted that the correlation between electrical conductivity and activation volume is preserved for all substances. Specifically, the activation volume decreases as the electrical conductivity increases. This probably reflects the similarity in transport mechanism for all substances studied.

Finally, it is of interest to compare the pressure results to those for solvent free ion-conducting polymers. A summary of the previous results for PPO are shown in Fig. 4 of Ref. 13 or Fig. 6 of Ref. 16 where it is seen that the activation volume decreases from about 80 to 20 $cm^3$/mol over the temperature range of about $70+T_0$ to $160+T_0$ °C. Data for PEO [45], amorphous PEO [27], and PDMS:EO [21,22] fall in the same range. Consequently, the results of about 12 to 17 $cm^3$/mol at about $138+T_0$ °C are somewhat smaller than the values observed for traditional ion-conducting polymers. This probably reflects the difference in transport mechanism between solvent free polymer electrolytes, where large scale segmental

motions control electrical transport, and the liquid and hybrid electrolytes studied in the present work.

## SUMMARY

In summary, several results have been obtained via NMR, DSC and electrical conductivity studies of various liquid and hybrid electrolytes. The liquids and hybrid electrolytes are similar in that the electrical conductivity of the EC:PC-based substances exhibits VTF (WLF) behaviour while that for the EC:DMC-based substances shows a rapid drop as temperature is lowered below about 250K. Further, the glass transition temperatures are about the same for each liquid and associated hybrid electrolyte. However, substantial differences are found. The electrical conductivity of the plasticized films at room temperature are lower than expected and, more importantly, the relative change of conductivity with pressure is larger than for the liquids. In addition, the NMR linewidth is larger for the hybrid electrolytes both above and below $T_g$. Also, above the glass transition temperature, the NMR $T_1$ values are smaller for the hybrid electrolytes than for the liquids. These differences, based on experiments with a dynamical range from d.c. to 100 MHz, suggest that the lithium ion motions are somewhat restricted in the hybrid electrolytes as compared with the bulk liquids. Consequently, it is concluded that significant solid matrix-lithium ion interactions take place.

*Acknowledgments*--This work was supported in part by the Office of Naval Research.

## REFERENCES


[1] A. S. Gozdz, J. -M. Tarascon, O. S. Gebizlioglu, C. N. Schmutz, P. C. Warren and F. K Shokoohi, Proceedings of the Symposium on Rechargeable Lithium and Lithium-ion Batteries, eds. S. Megahed, B. M. Barnett and L. Xie, Electrochemical Society, Pennington, NJ, 94-28 (1995) 400.

[2] J. -M. Tarascon, A. S. Gozdz, C. N. Schmutz, F. K Shokoohi, and P. C. Warren, Solid State Ionics 86-88 (1996) 49.

[3] M. Doyle, A. S. Gozdz, C. N. Schmutz and J. -M. Tarascon, J. Electrochem. Soc., 143 (1996) 1890.

[4] G. B. Appetecchi, F. Croce, B. Scrosati and M. Wakihara, Proceedings of the Symposium on Batteries for Portable Applications and Electric Vehicles, Electrochemical Society, Pennington, NJ, 97-18 (1997) 488.

[5] T. Skotheim, Appl. Phys. Lett. 38 (1981) 712.

[6] R. A. Zoppi, C. M. N. P. Fonseca, M. A. De Paoli and S. P. Nunes, Acta Polym. 48 (1997) 193.

[7] A. S. Gozdz, J. -M. Tarascon, C. N. Schmutz, P. C. Warren, O. S. Gebizlioglu and F. Shokoohi, Proc. Ann. Batt. Conf. Appl. Adv., eds. H. A. Frank and H. Oman, IEEE, New York, NY, 10 (1995) 301.

[8] C. Arbizzani, M. Mastragostino, L. Meneghello, X. Andrieu and T. Vicedo, Mater. Res. Soc. Symp. Proc., Solid State Ionics III 293 (1993) 169.

[9] K. Shigehara, N. Kobayashi and E. Tsuchida, Solid St. Ionics, 14 (1984) 85.

[10] X. -M. Wang, M. Iyoda, T. Nishina and I. Uchida, J. Power Sources, 68 (1997) 487.

[11] C. Borghini, M. Mastragostino, L. Meneghello, P. Manaresi and A. Munari, Solid St. Ionics, 67 (1994) 263.

[12] M. Oda and S. Higo, Patent: Jpn. Kokai Tokkyo Koho, JP 87278774 A2, JP 62278774, Date: 871203.

[13] A. Yamada and J. Shigehara, Patent: Jpn. Kokai Tokkyo Koho, JP 86254613, JP 61254613, Date: 861112.

[14] G. Feullade and P. Perche, J. Appl. Electrochem. 5 (1975) 63.

[15] E. Tsuchida, H. Ohno and K. Tsunemi, Electrochimica Acta 28 (1983) 591.

[16] K. Tsunemi, H. Ohno and E. Tsuchida, Electrochimica Acta 28 (1983) 833.

[17] Z. Jiang, B. Carroll and K. M. Abraham, Electrochimica Acta 42 (1997) 2667.

[18] J. J. Fontanella, M. C. Wintersgill, J. P. Calame, M. K. Smith and C. G. Andeen, Solid State Ionics 18&19 (1986) 253.

[19] J. J. Fontanella, M. G. McLin and M. C. Wintersgill, J. Polym. Sci.: Part B: Polym. Phys. 32 (1994) 501.

[20] Y. S. Pak, K. J. Adamic, S. G. Greenbaum, M. C. Wintersgill, J. J. Fontanella and C. S. Coughlin, Solid State Ionics 45 (1991) 277.

[21] M. C. Wintersgill, J. J. Fontanella, M. K. Smith, S. G. Greenbaum, K. J. Adamic and C. G. Andeen, Polymer 28 (1987) 633.

[22] K. J. Adamic, S. G. Greenbaum, M. C. Wintersgill and J. J. Fontanella, J. Appl. Phys. 60 (1986) 1342.

[23] J. J. Fontanella, M. C. Wintersgill, M. K. Smith, J. Semancik and C. G. Andeen, J. Appl. Phys. 60 (1986) 2665.

[24] J. J. Fontanella, C. A. Edmondson, M. C. Wintersgill, Y. Wu, S. G. Greenbaum, Macromolecules 29 (1996) 4944.

[25] C. A. Edmondson, M. C. Wintersgill, J. J. Fontanella, F. Gerace, B. Scrosatti and S. G. Greenbaum, Solid State Ionics 85 (1996) 173.

[26] S. G. Greenbaum, Y. S. Pak, M. C. Wintersgill, J. J. Fontanella, J. W. Schultz and C. G. Andeen, J. Electrochem. Soc. 135 (1988) 235.

[27] M. C. Wintersgill, J. J. Fontanella, Y. S. Pak, S. G. Greenbaum, A. Al-Mudaris and A. V. Chadwick, Polymer 30 (1989) 1123.

[28] J. T. Dudley, D. P. Wilkinson, G. Thomas, R. LeVae, S. Woo, H. Blom, C. Horvath, M. W. Juzkow, B. Denis, P. Juric, P. Aghakian and J. R. Dahn, J. Power Sources 35 (1991) 59.

[29] *Polymer Handbook*; Brandrup, J., Immergut, E. H., Eds.; John Wiley and Sons: New York 1975.

[30] J. Barthel, H. J. Gores, P. Carlier, F. Feuerlein and M.Utz, Ber. Bunsenges. Phys. Chem. 87 (1983) 436.

[31] A. Bondeau and J. Huck, J. Physique 46 (1985) 1717.

[32] C. A. Angell, J. Phys. Chem. Solids 49 (1988) 863.

[33] J. Huck, A. Bondeau, G. Noyel and L. Jorat, IEEE Trans. Electrical Insulation 23 (1988) 615.

[34] F. Stickel, E. W. Fischer and R. Richert, J. Chem. Phys. 105 (1996) 2043.

[35] C. A. Angell, Polymer 26 (1997) 6261.

[36] J. J. Fontanella et al., J. Power Sources, submitted.

[37] P.E. Stallworth, J. Li, S.G. Greenbaum, F. Croce, S. Slane and M. Salomon, Solid State Ionics, 73 (1994) 119.

[38]. H. Vogel, Physik Z., 22 (1921) 645; V. G. Tammann and W. Hesse, Z. Anorg. Allg. Chem., 156 (1926) 245; G. S. Fulcher, J. Amer. Ceram. Soc., 8 (1925) 339.

[39] J. J. Fontanella, M. C. Wintersgill, C. S. Coughlin, P. Mazaud and S. G. Greenbaum, J. Polymer Sci.: Polymer Phys. 29 (1991) 747.

[40]. M. L. Williams, R. F. Landel, and J. D. Ferry, J. Am. Chem. Soc., 77 (1955) 3701.

[41] J. T. Bendler and M. F. Shlesinger, J. Stat. Phys. 53 (1988) 531.

[42] P.E. Stallworth, S.G. Greenbaum, F. Croce, S. Slane and M. Salomon,

Electrochimica Acta, 40 (1995) 2137.

[43] S.G. Greenbaum, S. Panero and B. Scrosati, Electrochimica Acta, 37 (1992) 1533.

[44] F. Croce, S.D. Brown, S.G. Greenbaum, S.M. Slane and M. Salomon,Chem. Mater., 5 (1993) 1268.

[45] J. J. Fontanella, M. C. Wintersgill, J. P. Calame, F. P. Pursel, D. R. Figueroa and C. G. Andeen, Solid State Ionics 9&10 (1983) 1139.

TABLE 1. Summary of the the electrical conductivity and its pressure dependence for various electrolytes at room temperature.

| | $\sigma$ | $\frac{\partial \ln G}{\partial P}$ | $\chi_T$ | $\frac{\partial \ln \sigma}{\partial P}$ | $\Delta V$ |
|---|---|---|---|---|---|
| | mS/cm | $(GPa)^{-1}$ | $(GPa)^{-1}$ | $(GPa)^{-1}$ | $cm^3/mol$ |
| Film:EC:PC:$LiPF_6$ | 1.2 | -7.45 | 0.3 | -7.15 | 17.7 |
| EC:PC:$LiPF_6$ | 6.8 | -6.44 | 0.3 | -6.14 | 15.2 |
| | | | | | |
| Film:EC:DMC:$LiPF_6$ | 1.3 | -7.14 | 0.3 | -6.84 | 16.9 |
| EC:DMC:$LiPF_6$ | 11.5 | -5.35 | 0.3 | -5.05 | 12.5 |

TABLE 2. Best-fit VTF parameters for electrical conductivity data.

| Material | Temperature Range (K) | $\log_{10}(A'(S/cm))$ | B (eV) | $T_0$ (K) | RMS dev |
|---|---|---|---|---|---|
| Film:EC:PC:$LiPF_6$ | 196-296 | -1.03 | 602 | 157.3 | 0.0137 |
| EC:PC:$LiPF_6$ | 196-296 | -0.43 | 530 | 161.6 | 0.0211 |
| EC:PC:$LiPF_6$ | 190-296 | -0.296 | 579 | 158.7 | 0.0354 |

| | Temperature Range (K) | $\log_{10}(A(K^{1/2}S/cm))$ | B' (eV) | $T_0'$ (K) | RMS dev |
|---|---|---|---|---|---|
| Film:EC:PC:$LiPF_6$ | 196-296 | 0.285 | 634 | 156.3 | 0.0123 |
| EC:PC:$LiPF_6$ | 196-296 | 0.876 | 558 | 160.6 | 0.0190 |
| EC:PC:$LiPF_6$ | 190-296 | 1.00 | 605 | 157.9 | 0.0326 |

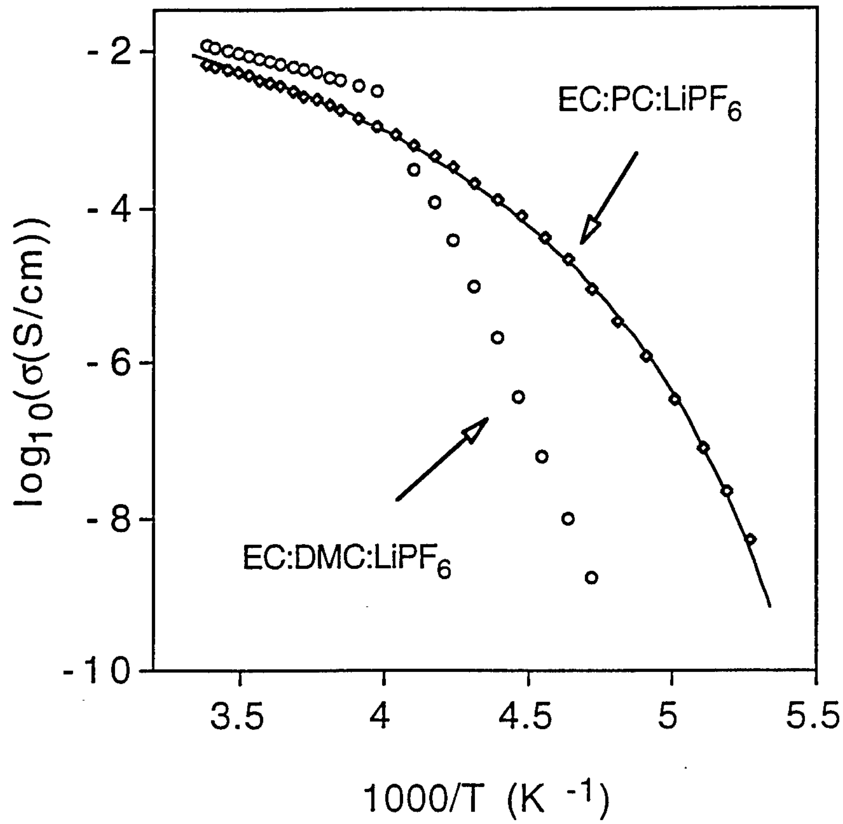


**Fig. 1.** Electrical conductivity vs. temperature for the liquid electrolytes: EC:PC:$LiPF_6$ (diamonds) and EC:DMC:$LiPF_6$ (circles). Also shown is the best-fit VTF curve (equation 4) for EC:PC:$LiPF_6$.

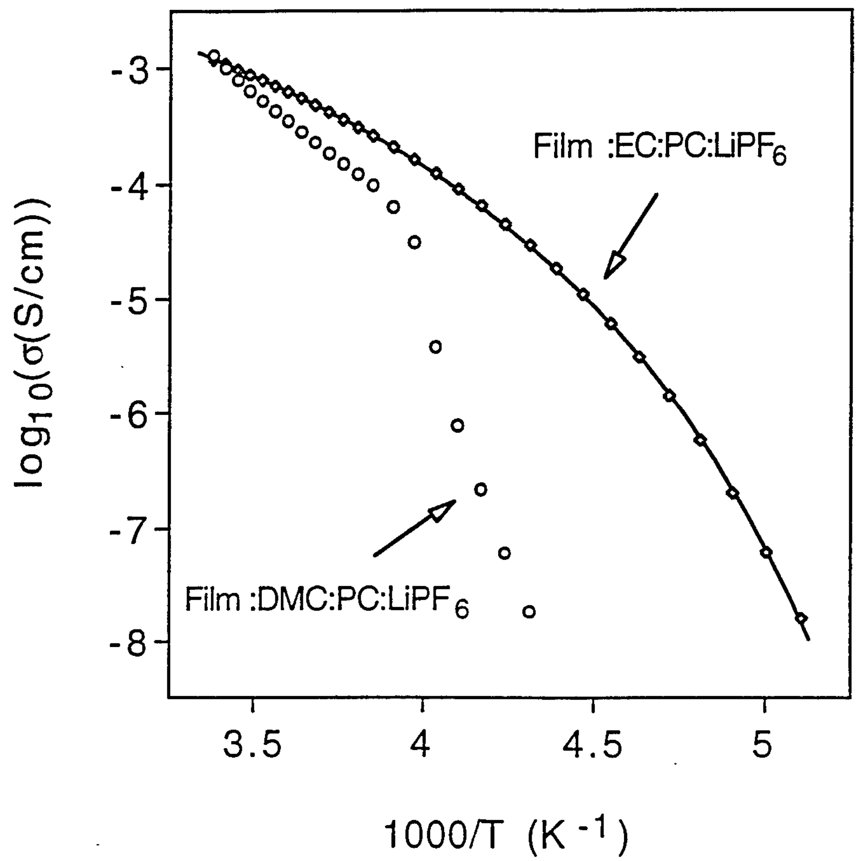


**Fig. 2**. Electrical conductivity vs. temperature for the hybrid electrolytes: Film:EC:PC:$LiPF_6$ (diamonds) and Film:EC:DMC:$LiPF_6$ (circles). Also shown is the best-fit VTF curve (equation 3) for Film:EC:PC:$LiPF_6$.

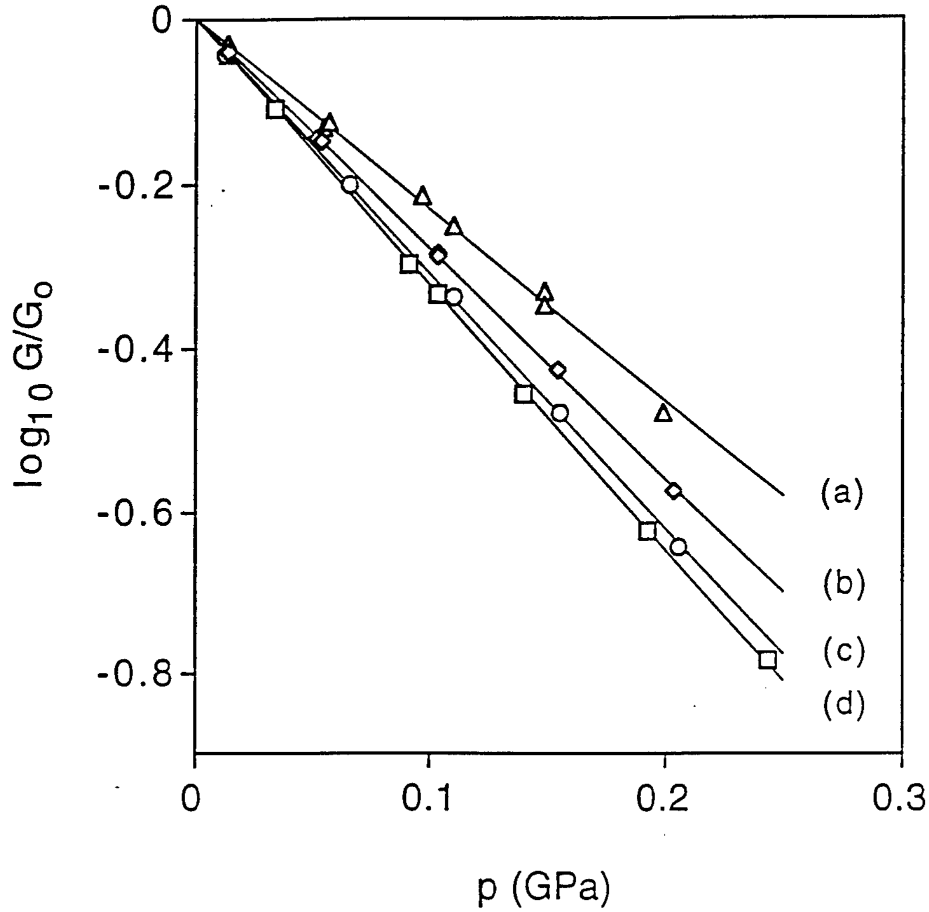


**Fig. 3.** Relative electrical conductance vs. pressures for (a) EC:DMC:$LiPF_6$; (b) EC:PC:$LiPF_6$; (c) Film:EC:DMC:$LiPF_6$; (d) Film:EC:DMC:$LiPF_6$. Also shown are the best-fit straight lines.

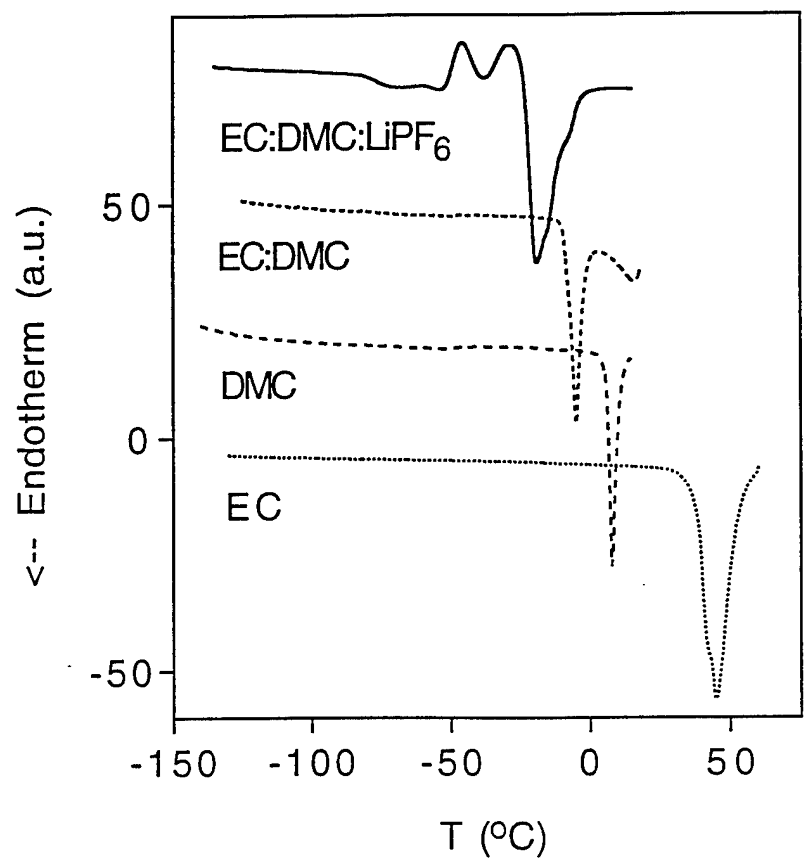


**Fig. 4.** DSC thermograms for EC, DMC, EC:DMC and EC:DMC:$LiPF_6$.

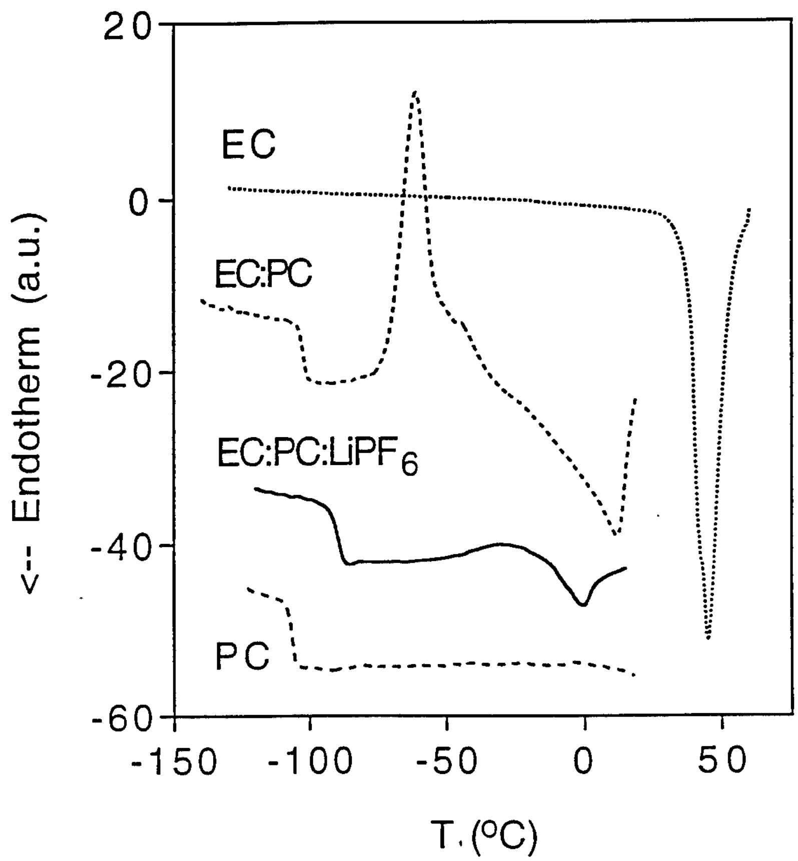


**Fig. 5.** DSC thermograms for EC, PC, EC:PC and EC:PC:$LiPF_6$.

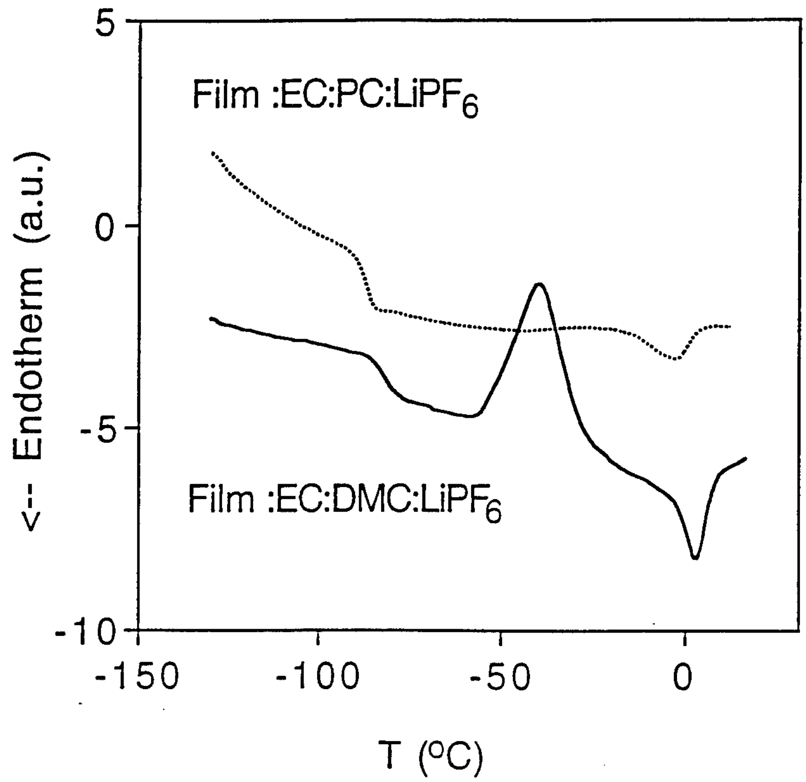


**Fig. 6.** DSC thermograms for Film:EC:DMC:$LiPF_6$ and Film:EC:PC:$LiPF_6$.

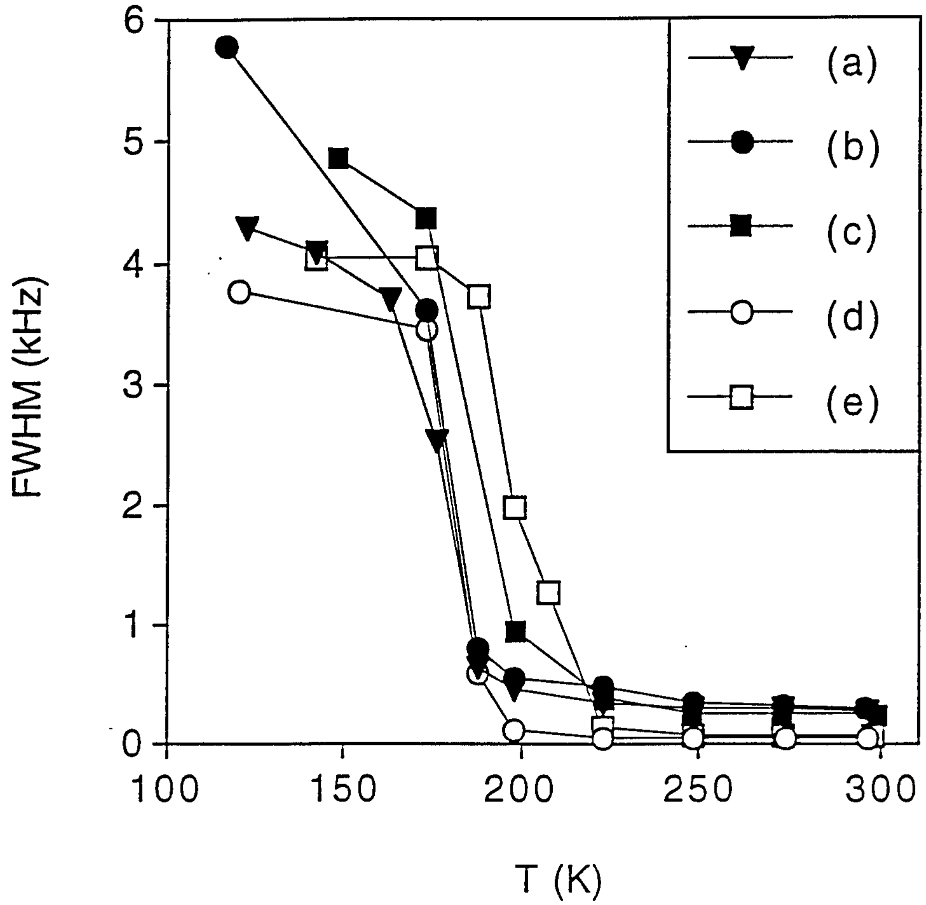


**Fig. 7.** $^{7}$Li linewidth for various materials: (a) Film:EC:PC:$LiCF_3SO_3$; (b) Film:EC:PC:$LiPF_6$; (c) Film:EC:DMC:$LiPF_6$, (d) EC:PC:$LiPF_6$; (e) EC:DMC:$LiPF_6$.

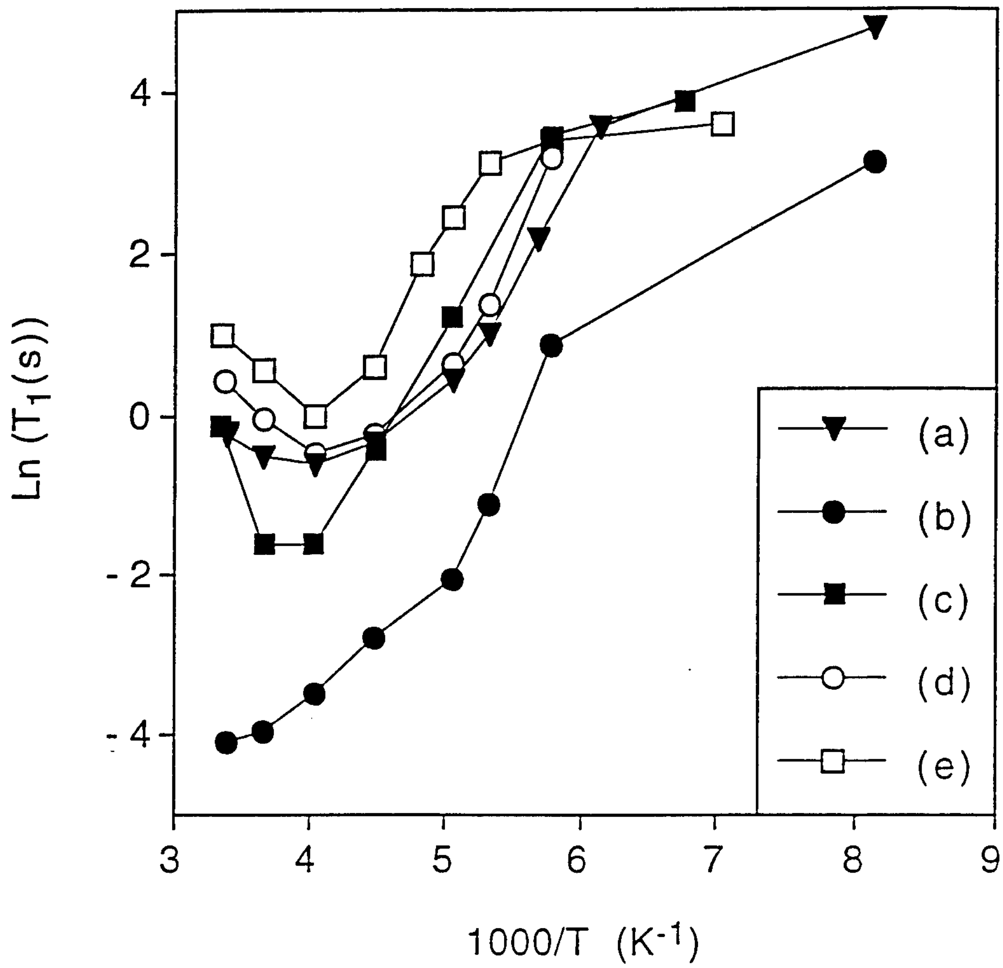


**Fig. 8.** Natural logarithm of $^7$Li spin-lattice relaxation time ($T_1$) vs. 1000/T for various materials: (a) Film:EC:PC:$LiCF_3SO_3$; (b) Film:EC:PC:$LiPF_6$; (c) Film:EC:DMC:$LiPF_6$, (d) EC:PC:$LiPF_6$; (e) EC:DMC:$LiPF_6$.